# Fabrication of Low-Density Foam Shells from Resorcinol–Formaldehyde Aerogel

STEPHEN M. LAMBERT,[1] GEORGE E. OVERTURF, III,[2] GERALD WILEMSKI,[2] STEPHAN A. LETTS,[2] DIANA SCHROEN-CAREY,[3] ROBERT C. COOK[2]

[1] Soane Technologies, Inc., 3916 Trust Way, Hayward, California 94545

[2] Lawrence Livermore National Laboratory, P.O. Box 808, Livermore, California 94551

[3] W. J. Schafer Associates, 303 Lindbergh Avenue, Livermore, California 94550

*Received 12 July 1996; accepted 10 January 1997*

**ABSTRACT:** Resorcinol–formaldehyde (RF) aerogel chemistry has been used with encapsulation techniques to fabricate low-density, transparent, foam shells. To accomplish this, the gelation time was reduced from several hours to several minutes by the addition of acid following base-catalyzed RF particle growth. However, additional "annealing" of the gel for at least 20 h was needed to maximize crosslinking and minimize swelling in exchange solvents. Increasing the molar ratio of formaldehyde to resorcinol from 2 to 3 also helped to increase crosslinking. Densification of the foam shells due to dehydration during curing was greatly reduced by judicious choice of immiscible oil phases and by saturating the exterior oil phase during the annealing stage. Shells have been produced with diameters of about 2 mm, wall thicknesses ranging from 100 to 200 $\mu$m and foam densities approaching 50 mg/cc. © 1997 John Wiley & Sons, Inc. J Appl Polym Sci **65:** 2111–2122, 1997

**Key words:** resorcinol; formaldehyde; organic aerogel; encapsulation; ICF

## INTRODUCTION

Future inertial confinement fusion (ICF) targets at the University of Rochester Laboratory for Laser Energetics and for the planned National Ignition Facility will require 1 to 2 mm diameter spherical organic polymer shells with an 80–100 $\mu$m thick cryogenic liquid or solid layer of deuterium-tritium (DT) on the inside surface.[1,2] A potential route to this goal is to line the inside of the target with a layer of low-density ($\sim$ 50 mg/cm$^3$), low-atomic-number foam that helps support and symmetrize the fuel.[3] This article describes the fabrication of this inner foam mandrel via the encapsulation of resorcinol–formaldehyde (RF) aerogel.

The preparation of foam shells by encapsulation was first developed by Takagi et al.[4–8] using a methacrylate-based chemistry. In their scheme, an aqueous drop is enclosed by an immiscible organic solvent shell; this compound drop is, in turn, immersed in a continuous aqueous phase. After formation of the compound drop, a multifunctional methacrylate monomer dissolved in the organic phase undergoes free radical polymerization to create a crosslinked gel that occupies the volume of the organic phase. After polymerization is complete, the water and organic solvent are exchanged with a mutually miscible solvent; this solvent (typically ethanol or 1,4-dioxane) is then exchanged with liquid carbon dioxide ($CO_2$). Dry

*Correspondence to*: Robert C. Cook.

Contract support: U.S. Department of Energy, contract number: W-7405-ENG-48 (Lawrence Livermore National Laboratory) and contract number: DE-AC03-9SSF20732 (W. J. Schafer Associates and Soane Technologies).

Journal of Applied Polymer Science, Vol. 65, 2111–2122 (1997)
 CCC 0021-8995/97/112111-12

foam shells are obtained by removing the $CO_2$ as a supercritical fluid.

This work[4–8] and subsequent work performed at the Lawrence Livermore National Laboratory on methacrylate-based foam shells[9] revealed two important features of the encapsulation technique. First, gelation of the shell phase must occur quickly to stabilize the inherently unstable compound drop. Second, the densities of the inner droplet and that of the shell phase containing the polymerizable monomer must be carefully matched to eliminate buoyancy effects that can further destabilize the drop as well as lead to nonuniform shell wall thickness.

The impetus to pursue shells made of resorcinol–formaldehyde aerogel was provided by its considerably greater optical transparency compared to methacrylate-based foams.[10] The opacity of methacrylate foams is due primarily to the scattering of light by the relatively large, 1–3 $\mu$m, cell structure.[11] RF aerogel, on the other hand, has a cell size on the order of 0.1 $\mu$m and is significantly more transparent than the methacrylate foams.

The preparation of RF foams differs considerably from that of methacrylate-based foams, and these differences profoundly affect the encapsulation process. One important difference is that the typical gelation time of conventional RF aerogel formulations is many hours.[12–18] Because successful encapsulation is possible only if gelation of the shell phase occurs within 15 to 20 min, a means of accelerating gelation is needed that can maintain the desired foam properties (e.g., transparency and low density). Another important difference is that, in the case of the RF system, polymerization occurs in an aqueous medium rather than an organic ("oil") medium. As a result, an oil-in-water-in-oil system is needed to create RF aerogel shells rather than the water-in-oil-in-water system used for methacrylate foam shells.

This article is organized as follows: in the next section we briefly review the chemistry, processing and properties of bulk RF aerogel; this leads to a description of our method for significantly reducing the gelation time. In the two sections after this, the effectiveness of this method is examined by viscometry studies and the response of RF gels to solvent exchanges. In the next to last section we describe various aspects of encapsulating this material to create shells. These aspects include formation of the oil-in-water drop, selecting appropriate exterior and interior oil phases, and minimizing dehydration of the aqueous layer during gelation. In the last section we compare the behavior of the shells during solvent exchanges and drying to that of the bulk aerogel.

## RF AEROGEL CHEMISTRY

The use of resorcinol–formaldehyde resin chemistry to form low-density microcellular materials was pioneered by Pekala et al.[12–14] In basic aqueous solutions at elevated temperatures (60–95°C), resorcinol and formaldehyde react to form crosslinked nanometer-sized particles. After the initial particle formation and growth stage, which can take several hours, the colloidal particles begin to aggregate and assemble into a stiff interconnected structure locally resembling a "string of pearls" that fills the original volume of the aqueous solution.

A supercritical $CO_2$ drying technique is used to preserve the fine scale cellular structure of the foam. In addition, because we wish to have tight control over the dimensions of the final dry shell, we also require that the gel be sufficiently stiff and crosslinked so that it does not undergo any dramatic dimension changes (i.e., swelling or shrinking) during solvent exchanges and drying.

RF formulations are characterized by three quantities related to the initial composition of the aqueous solution. The first is the molar ratio of formaldehyde to resorcinol (F/R). A ratio of 2 has been used in all previous studies,[12–18] but we have investigated the effect of increasing it to 3. The ortho- and para-directing effects of resorcinol's hydroxyl groups allow the addition of formaldehyde to the 2-, 4-, and/or 6-ring positions resulting in methylol substituted resorcinol. Increasing F/R should increase the average functionality of the substituted resorcinol and, ultimately, the degree of crosslinking.

The second quantity is the molar ratio of resorcinol to "catalyst" (R/C). The catalyst in this reaction is sodium carbonate, which deprotonates a small fraction of the resorcinol. Resorcinol anions act as sites for the growth of RF particles because they are more reactive with formaldehyde than neutral resorcinol molecules. Reducing R/C (i.e., increasing the catalyst concentration) produces more particles of smaller size. Investigation here is limited to R/C ratios of 100 and 200 because it is known that these yield the lowest density and most optically transparent foams.[12–15]

The last quantity is the "theoretical" dry foam density, which is determined from the concentra-

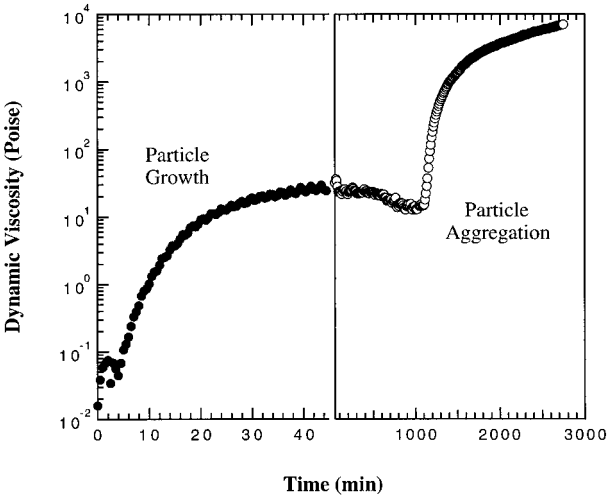


**Figure 1** Dynamic viscosity of an RF solution (30 mg/cm$^3$ theoretical foam density, F/R = 2, R/C = 100) at 70°C. The first regime corresponds to particle growth. The second regime corresponds to particle aggregation to form the stiff gel. Note change in time scale between regimes on the horizontal axis. From Letts et al.[15].

tion of polymerizable reactants (resorcinol and formaldehyde) in the initial aqueous solution. Because the density of water is approximately 1 g/cm$^3$, a solution containing a combined 5 wt % of resorcinol and formaldehyde will have a theoretical density of about 50 mg/cm$^3$. Due to some shrinkage of the gel upon drying, actual foam densities are usually slightly higher than the theoretical densities. Pekala et al.[12] found that the minimum amount of shrinkage for gels with F/R = 2 occurs when R/C = 200. We have worked primarily with RF formulations that produce foams with theoretical densities of 50 and 75 mg/cm$^3$.

Letts et al.[15] have shown by dynamic viscosity measurements that the base-catalyzed RF reaction at 70°C is initially dominated by particle growth, which typically ceases after about 1 h. This is illustrated in Figure 1 by the initial rise and plateauing of the dynamic viscosity at a relatively low value. At some point many hours later (note change in scale), a second large increase in the dynamic viscosity signals the aggregation of particles to form a stiff gel. Titration measurements[16] show that most of the formaldehyde is consumed within the first half hour. These results coupled with light-scattering studies[17,18] provide convincing evidence that particle growth is completed well before aggregation begins.

It is our belief that the two regimes are a manifestation of changes in pH. We have measured the pH of an RF solution and, as shown in Figure 2, found that it becomes more acidic over approximately the same time period as formaldehyde consumption and RF particle growth. During the particle growth stage, base catalyzes the formation of methylene bridges between substituted resorcinols, generating enough acid to gradually reduce the pH. After particle growth has stopped, links between particles are created by the acid-catalyzed reaction between methylol groups on the surfaces of particles to form methylene–ether bridges. NMR studies[14] support this difference between intra- and interparticle bridging structure. Because the solution is typically only slightly acidic after particle growth, aggregation proceeds at a slow rate. Thus, we reasoned that artificially lowering the pH by adding acid should more rapidly aggregate the particles to the point of gelation.

This hypothesis has been confirmed experimentally. Figure 3 shows the dynamic viscosity when sufficient benzoic acid was added, following 1 h of conventional base-catalyzed reaction, to reduce the pH to about 4. After a short period, the dynamic viscosity rapidly increases and plateaus in as little as 2 h. This leads to the "two-step" procedure outlined in Figure 4 for preparing and curing RF gels. First, requisite amounts of the reactants are mixed together and heated to 70°C while stirring for 1 h. Afterwards, the solution is cooled for several minutes in an ice-water bath and 20 mL of a 1.8 g/L aqueous solution of benzoic acid is

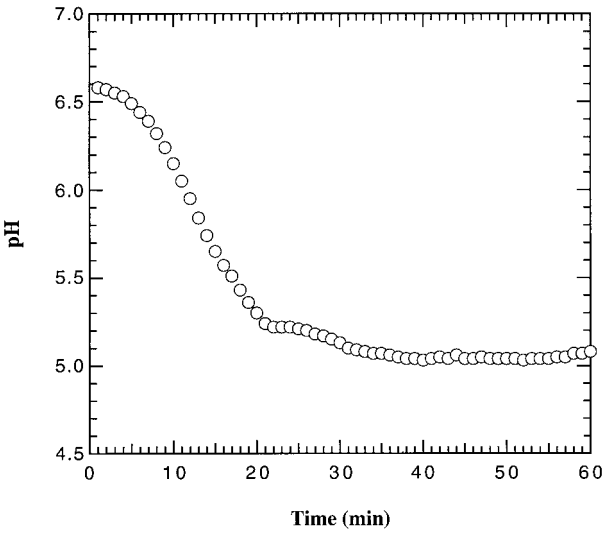


**Figure 2** pH of an RF solution (50 mg/cm$^3$ theoretical foam density, F/R = 2, R/C = 200) during the first hour of base-catalyzed reaction at 70°C.

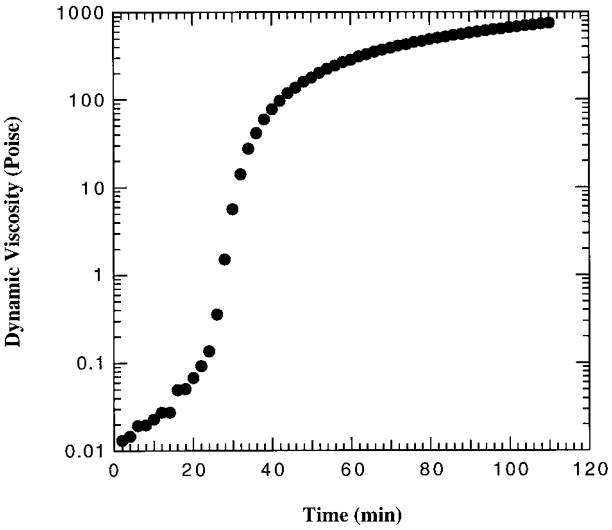


**Figure 3** Dynamic viscosity of an RF solution (50 mg/cm$^3$ theoretical foam density, F/R = 2, R/C = 200) at 70°C, which has been spiked with 0.026 wt % benzoic acid following 1 h of conventional base-catalyzed reaction.

added. Gelation occurs upon reheating the solution to 70°C. To ensure that the theoretical density of the gel remains 50 mg/cm$^3$ after the addition of benzoic acid solution, 20 mL of water is withheld during base catalysis. Encapsulation to form shells is performed after the addition of acid prior to the final cure.

## VISCOMETRIC STUDY OF ACID-ACCELERATED RF GELATION

To optimize this two-step RF polymerization process, we studied the effects of modifying some of the concentrations and conditions outlined in Figure 4. These include R/C, the length of the initial

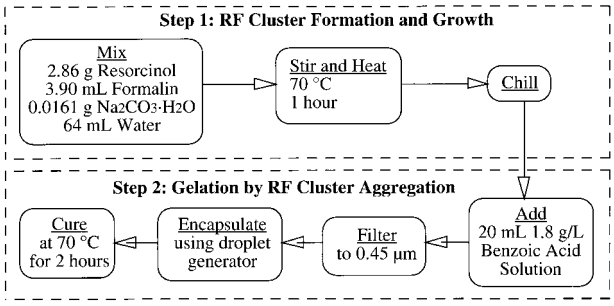


**Figure 4** The two-step process for preparing acid-accelerated RF gels (50 mg/cm$^3$ theoretical foam density, F/R = 2, R/C = 200).

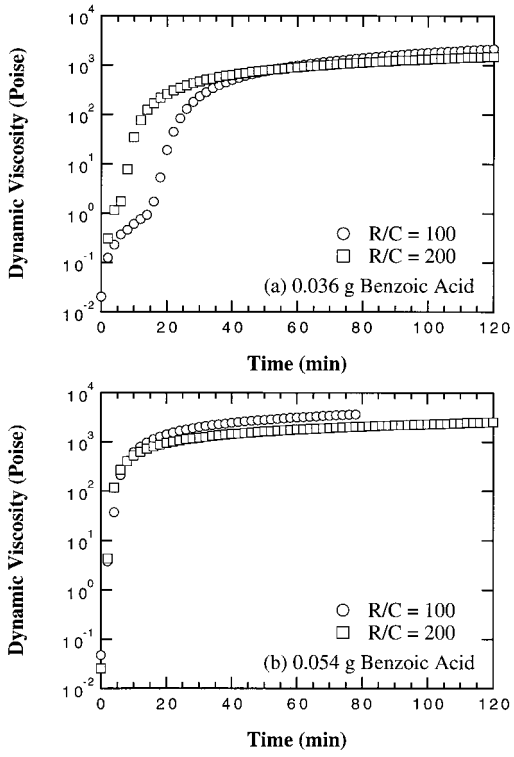


**Figure 5** Dynamic viscosity of RF solutions (50 mg/cm$^3$ theoretical foam density, F/R = 2) during cure at 70°C as a function of R/C and amount of benzoic acid added.

base-catalysis period, and the amount of benzoic acid added. For all solutions F/R = 2. The goal of this study was to decrease the gelation onset time and maximize the dynamic viscosity of the gel after curing for 2 h. The former gives some indication of how long it takes the gel to "set," and the latter gives an indication of the strength and stiffness of the material. The dynamic viscosity was measured using a Rheometrics fluid spectrometer in a couette geometry with an applied strain of 5% at a frequency of 10 rad/s.

To vary the amount of benzoic acid added, 40 mL water (as opposed to only 20 mL) was withheld during the initial base catalysis. The amount of benzoic acid was varied by adding 20 or 30 mL of benzoic acid solution and making up the remaining volume by adding pure water. The formulation can then be characterized simply by the mass of benzoic acid added to the solution.

Figure 5 shows the effect of varying the acid content on the dynamic viscosity of formulations with different values of R/C. Both the R/C = 100 and R/C = 200 solutions were base catalyzed for 1 h. For both values of R/C, increasing the acid

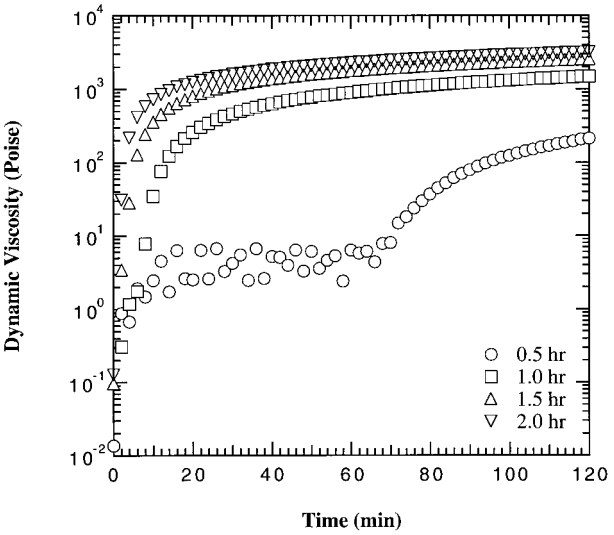


**Figure 6** Dynamic viscosity of RF solutions (50 mg/cm$^3$ theoretical foam density, F/R = 2, R/C = 200, 0.036 g benzoic acid added) during cure at 70°C as a function of base catalysis time.

concentration "sets" the gels more rapidly and increases the plateau viscosity. The increases in gelation rate with acid content is consistent with our assumption that acid catalyzes the reaction that forms methylene–ether bridges between methylol groups on the surfaces of RF particles.

For a given amount of benzoic acid, understanding the effect of changing R/C is not as straightforward. RF solutions become more basic as R/C is decreased. Due to the increased basicity, more of the added acid will neutralize the carbonate rather than promote aggregation. As a result, a given amount of acid will be less effective in promoting gelation in low R/C solutions than high R/C solutions. This is most evident in Figure 5(a) when 0.036 g of benzoic acid is added; as R/C decreases, the gelation onset time is shifted to longer times. Despite delaying the onset of gelation, gels with lower R/C plateau at a slightly higher viscosity. As shown in Figure 5(b) for solutions with higher acid contents, the effect of differences in R/C become less distinguishable.

Figure 6 shows the effect of varying the length of the initial base-catalysis period. The viscosity behavior is significantly affected within the first hour; after 0.5 h, particle growth is probably still occurring. The increases in gelation rate and plateau viscosity when base-catalysis time is extended beyond 1 h are probably due to continued intraparticle crosslinking and the start of some aggregation before acid addition. Increasing the base-catalysis time has a similar effect as increasing acid content; hence, for longer base-catalysis periods, less acid is needed to accelerate gelation.

Figure 7 shows the effect of reactant concentration during base catalysis for RF solutions that were base catalyzed for 1 h with identical acid content. The reactant (resorcinol and formaldehyde) concentrations were altered by withholding various amounts of water until after the base-catalysis period. The water volumes listed are those present during base catalysis. More rapid gelation and higher plateau viscosity can be achieved by diluting concentrated solutions following base catalysis. This result is most likely a manifestation of increased reaction rates in more concentrated solutions.

## SWELLING OF RF GELS IN ISOPROPANOL

After the gels are cured, they are dried by first replacing the water solvating the gel with isopropanol (IPA). The gels in IPA are then placed in a temperature-controlled pressure vessel where the IPA is replaced with liquid $CO_2$. IPA was chosen as the intermediate solvent because it is miscible with both water and liquid $CO_2$. The fixed-volume vessel is then heated and pressurized above the critical point of $CO_2$ (31°C and 71 atm). The $CO_2$ is removed by depressurizing the vessel

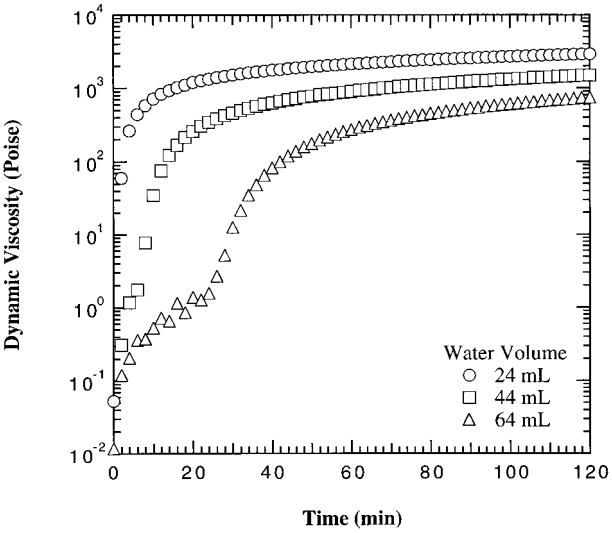


**Figure 7** Dynamic viscosity of RF gels (50 mg/cm$^3$ theoretical foam density, F/R = 2, R/C = 200, 0.036 g benzoic acid added) during cure at 70°C as a function of the volume of water present during base catalysis for 1 h.

at constant temperature ($\approx 40°C$) to atmospheric pressure to leave the dry aerogel.

When gels were cured for 2 h and "exchanged" into IPA, macroscopic swelling was observed, which suggested they were not sufficiently crosslinked. Due to the colloidal nature of the gel structure, there are two types of crosslinks: intraparticle crosslinks within the nanometer-sized particles comprising the gel matrix, and interparticle crosslinks. Swelling most likely emanates from the former, because swelling is indicative of a molecular-level interaction between the polymer and solvent. It seems unlikely that the swelling results from reorganization of the chemically linked particles into an expanded structure. The most obvious way to increase intraparticle crosslinking is simply to increase the curing time.

Consequently, the degree of swelling of bulk RF gels in IPA was measured as a function of cure time. We also investigated the influence of R/C and F/R on swelling. After acid additions, RF solutions were sealed in 10 mL glass ampoules. The filled ampoules were heated to 70°C for periods ranging from 1.5 to 30 h. Afterwards, they were placed in ice water to quench reactions. The cylindrical gels were removed from the ampoules, cut into four to five pieces, placed in water, and their diameters measured. After measurement, the gels were exchanged into IPA and their dimensions measured again.

If the swelling of the gel is isotropic, the degree of swelling, ($\Delta V/V$), can be estimated as

$$\frac{\Delta V}{V} \equiv \frac{V_{\mathrm{IPA}} - V_w}{V_w} = \left(\frac{d_{\mathrm{IPA}}}{d_w}\right)^3 - 1 \qquad (1)$$

where $V_w$ and $d_w$ are the volume and diameter of the gel in water, respectively, and $V_{\mathrm{IPA}}$ and $d_{\mathrm{IPA}}$ are the volume and diameter of the gel after exchanging into IPA.

Swelling results are summarized in Figure 8. The most significant observation is that large changes in gel dimensions after exchanging into IPA can only be avoided by curing the gel for at least 20 h, rather than the 2 h suggested by the dynamic viscosity measurements. R/C and F/R also influence swelling. For a given F/R, gels prepared with R/C = 100 swell less than gels with R/C = 200. Lowering R/C results in the growth of smaller particles, which are probably more crosslinked. For a given R/C and long curing times, swelling can be reduced further by increasing F/R from 2 to 3, which promotes intraparticle crosslinking by increasing the average functionality of methylol substituted resorcinol moieties.

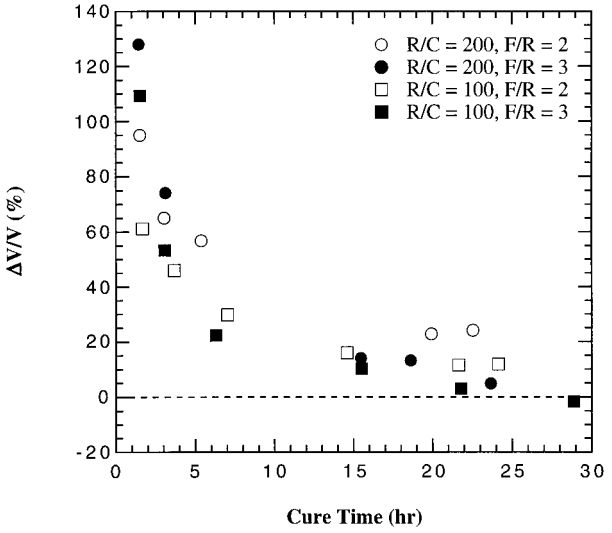


**Figure 8** Degree of swelling of bulk RF gels (50 mg/cm$^3$ theoretical foam density) in isopropanol as a function of cure time at 70°C for several combinations of F/R and R/C.

In summary, this study of RF chemistry, viscometry, and swelling provided important information needed to encapsulate the RF material. By spiking the RF solutions with an appropriate amount of acid following the base-catalyzed particle growth stage, the gelation times can be reduced from many hours to less than 20 min. However, although the macroscopic interparticle gel structure sets in minutes, additional "annealing" of the gel is needed for up to 20 h to maximize intraparticle crosslinking and thus minimize swelling in exchange solvents.

## ENCAPSULATION METHOD, SOLVENTS, AND CURING

Encapsulation of RF solutions to form a spherical shell is accomplished by using a triple-orifice droplet generator. The generator and preformed RF shells ("preforms") are shown schematically in Figure 9. The preforms consist of an interior oil-phase droplet that is surrounded by the ungelled aqueous RF solution. This compound drop is formed from two concentric orifices that are inserted into a tube (the "third" orifice) through which flows a second, exterior oil phase. The droplets are stripped off the inner orifices by the axial flow of the exterior oil phase. The delivery tube

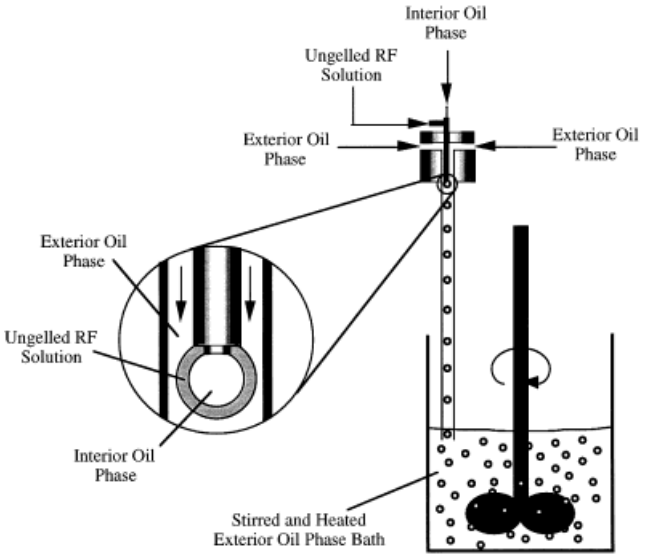


**Figure 9** Schematic diagram of the triple-orifice droplet generator.

(≈ 10 cm in length) is made from Teflon to provide a hydrophobic surface that is wetted only by the exterior oil phase. The diameter of the shell is roughly determined by the diameter of the delivery tube. More precise adjustment of the diameter is achieved by adjusting the exterior oil phase flow rate. The wall thickness of the shell is determined by the ratio of the interior oil phase and RF solution flow rates.

The preformed shells flow down the delivery tube into a gently stirred, heated beaker containing about 150 mL of the exterior oil phase. Agitation of the shells is necessary to maintain drop sphericity. Agglomeration and coalescence of the preformed shells is reduced by the addition of about 0.1 wt % of SPAN 80 surfactant to the exterior oil phase. Approximately 200–300 shells are created by the droplet generator per batch, of which one-third to two-thirds survive the curing step.

The choice of appropriate interior and exterior oil phases was not immediately obvious. The only initial requirements were that they be immiscible with water and that the interior phase be closely matched in density to the aqueous RF phase to minimize wall thickness nonuniformity. Dibutyl phthalate was chosen initially for the outer oil phase because it was used for the preparation of methacrylate foam shells.[8,9] For density matching reasons, 1-methyl naphthalene was chosen as the interior oil phase because its density is closer to that of the RF solution than is dibutyl phthalate's. The density of the exterior oil phase is also important, but for a different reason. Its density should only be slightly less than that of the compound drops to help keep them suspended without applying vigorous agitation.

In retrospect, dibutyl phthalate was a poor choice for the exterior oil phase. Initial results[10] showed that shell walls thinned during cure due to a decrease in the volume of the aqueous phase. This dehydration resulted in shells with foam densities that were two to three times greater than the theoretical foam density. Although nearly immiscible with water, dibutyl phthalate has enough capacity to dissolve much of the water present in the preformed shells. The solubility of water in dibutyl phthalate at 25°C is 0.46 wt %.[19] The dibutyl phthalate (as received) was determined by Karl-Fischer titration to contain 0.12 wt % water. Hence, 150 mL of dibutyl phthalate has the capacity to absorb about 0.5 g of water, which is about half the water present in 100 compound drops. This situation is exacerbated at the higher temperatures needed to cure the RF gel. Saturating the exterior oil phase with water before attempting encapsulation failed because it severely reduced the effectiveness of the surfactant.

We examined factors that control the transport of water from the shell into the exterior oil phase using a model for convectively enhanced mass transfer from an isolated aqueous shell suspended in an agitated nonaqueous solvent. According to the model (detailed in the Appendix) the rate of water lost from the shell can be written as

$$\frac{df}{dt} \propto \frac{k_s T^{2/3} \omega^{1/2}}{\delta \mu^{5/6}} \qquad (2)$$

where $f$ is the fraction of water removed from the shell, $t$ is time, $k_s$ is the partition coefficient of water between the RF solution and the oil phase, $T$ is temperature, $\omega$ is related to the degree of solution agitation, $\delta$ is the shell wall thickness, and $\mu$ is the viscosity of the oil phase. The relatively weak dependence on the oil phase density and molecular weight have been omitted. Equation (2) points out the desirable properties and processing conditions that help to reduce shell dehydration. First, the rate of water transport out of the shell is directly proportional (through $k_s$) to the solubility of water in the organic oil phase. Second, eq. (2) suggests curing at lower temperatures and reduced agitation. Third, shells with thinner walls are more susceptible to dehydration

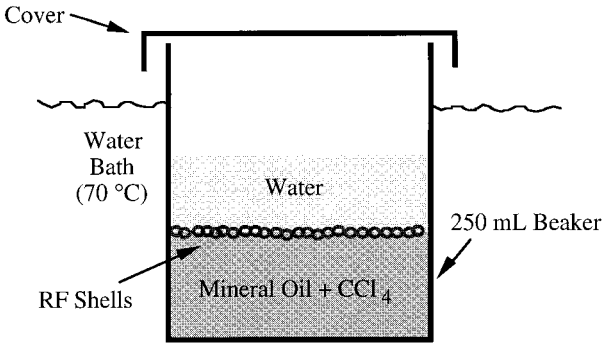


**Figure 10** Configuration for "annealing" gelled RF shells for long periods.

than thick-walled shells. Fourth, oil phases with higher viscosity will retard water transport out of the shell.

This analysis led us to consider a grade of mineral oil commonly known as Nujol oil. This fluid has a very low water solubility (0.0038 wt % at 25°C) that is more than two orders of magnitude smaller than that of dibutyl phthalate. Compared to other fluids with similar water solubility (e.g., dodecane), mineral oil has a significantly higher viscosity. However, a major drawback is that its density (0.85 g/cm$^3$ at 25°C) is too low to keep the shell preforms adequately suspended. This problem can be circumvented by sacrificing some of the higher viscosity of the mineral oil by mixing it with about 40 wt % carbon tetrachloride, which has a high density and a comparably low water solubility (1.59 g/cm$^3$ and 0.011 wt % at 25°C).

It was observed that stripping shell preforms off the inner orifices is best achieved with pure mineral oil rather than the mineral oil/carbon tetrachloride mixture. As a result, pure mineral oil (without surfactant) is used as the stripping phase in the droplet generator, which then flows into the gently stirred and preheated mixture of mineral oil, carbon tetrachloridem and surfactant. This mixture is held at 70°C and the shells are allowed to cure for 1.5–2 h. Compared to results found using dibutyl phthalate, the amount of densification due to dehydration during this period was noticeably reduced. However, although 1.5–2 h is enough time to stabilize and stiffen the shell preforms, water evaporation from the system becomes the dominant mechanism for additional water loss over the remaining 20–22 h of cure needed to maximize intraparticle crosslinking.

To avoid dehydration of the shells over longer times, the gelled shells are "annealed" in the configuration shown schematically in Figure 10. After the initial 1.5–2 h of cure, the preforms have "hardened" enough that agitation is no longer required; when agitation stops, the shells sink to the bottom of the beaker. One-half to one-third of the mineral oil/carbon tetrachloride mixture is decanted off and additional carbon tetrachloride (about 5–10 mL) is added until the shells float near the surface. Some water (50–75 mL) is then placed on top of the denser oil phase, which saturates the oil phase and prevents further dehydration of the shells. Finally, the beaker is covered and placed in a 70°C constant temperature bath for an additional 20–22 h.

## SOLVENT EXCHANGE, DRYING, AND CHARACTERIZATION

During the "annealing" period, the shells eventually sink to the bottom of the beaker due to permeation of carbon tetrachloride from the exterior oil phase through the aqueous layer into the 1-methyl naphthalene interior-oil phase. This helps separate shells from residual RF debris (broken and collapsed shells), which tends to remain at the oil/water interface. This separation allows the water, residual RF, and most of the oil phase to be decanted off, leaving the shells behind. Surviving shells are soaked in IPA to dissolve excess exterior oil phase, replace the water solvating the gel, and replace the interior oil phase. After numerous exchanges with fresh IPA, the shells are ready to be dried by the supercritical drying technique.

Some shells, particularly those with very nonuniform wall thickness, can dimple or deform during the exchange into IPA. Shells prepared using 75 mg/cm$^3$ RF formulations were more robust during exchanges than shells prepared from 50 mg/cm$^3$ formulations. Annealed shells prepared from both formulations appear to swell more in IPA than the corresponding bulk RF gels. Reliable optical measurement of individual shell swelling was not possible because differences in the refractive indices of the various fluids surrounding the shell give misleading values of the shell wall thickness.

The consistency of shell dimensions and wall thickness within a batch is illustrated in Figure 11. The droplet generator has the capacity to make shells whose dimensions (in IPA) range from 1.6 to 2.3 mm in diameter and from 100 to 200 $\mu$m in wall thickness. The deviation of diameters and wall thicknesses within a batch of shells

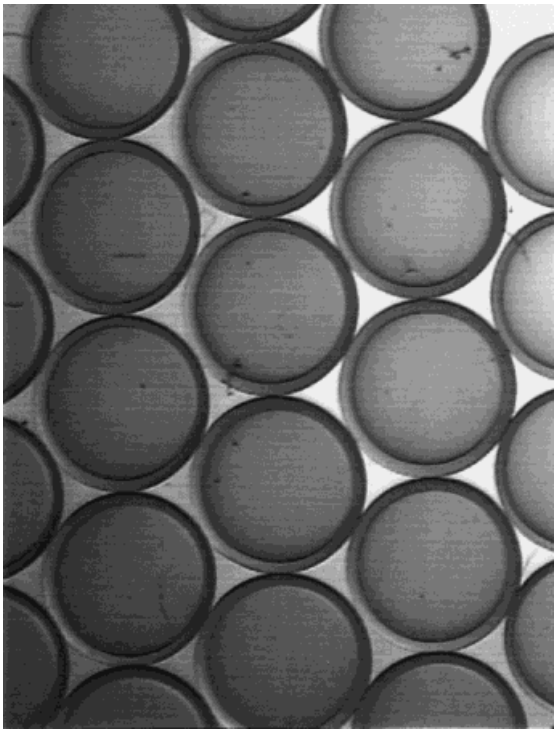

**Figure 11** A typical batch of RF shells after exchange into isopropanol. The average diameter and wall thickness for this batch are 2.3 mm and 145 $\mu$m, respectively.

is typically $\pm$0.03 mm and $\pm$10 $\mu$m, respectively. In general, the inner and outer shell walls were more concentric for 75 mg/cm$^3$ RF formulations than 50 mg/cm$^3$ RF formulations, suggesting that the latter were not as well density matched with the interior oil phase.

The measured foam densities of shells is compared to that of bulk RF aerogel in Table I. Shells and bulk samples prepared with F/R = 2 and R/C = 100 have higher densities than samples prepared with F/R = 2 and R/C = 200. This observation is consistent with an earlier finding[12] that R/C = 100 gels shrink more upon drying than R/C = 200 gels. This trend is also observed when F/R is increased to 3, despite the fact that these gels swell less in IPA. Hence, with respect to dimensional changes during processing, RF formulations with F/R = 3 and R/C = 200 are optimal. In all cases, the dry foam density of shells is consistently larger than that of the bulk foam, and this is a likely indication that some unavoidable dehydration of the shells by the oil phase solvents is still occurring. These results differ slightly from previous results[12] in that the measured density of the bulk R/C = 200 gels is slightly less than the theoretical density. This would only be possible if the reactants were not completely polymerized or swelling was retained after drying. Measured dimensions of the dry gels indicate the latter not to be the case. The removal of unreacted components is more likely, especially for gels prepared with higher formaldehyde contents.

**Table I Measured Dry Foam Densities of RF Shells and Bulk RF Aerogel as a Function of R/C and F/R**

| Sample Description | Measured Density (mg/cm$^3$) |
|---|---|
| R/C = 100, F/R = 2 | |
| Bulk | 73 |
| Shells | 80 |
| R/C = 100, F/R = 3 | |
| Bulk | 55 |
| Shells | 65 |
| R/C = 200, F/R = 2 | |
| Bulk | 47 |
| Shells | 64 |
| R/C = 200, F/R = 3 | |
| Bulk | 48 |
| Shells | 60 |

The theoretical density of all samples is 50 mg/cm$^3$.

Dry foam shells have also been examined by optical and scanning electron microscopy (SEM). Figure 12 is a photo of a dry shell placed on top of a ruler with 1 mm division. This photo clearly demonstrates the optical transparency of the aerogel and provides a visual indication of the uniformity and sphericity of the wall that can be achieved. SEM analyses of a fractured shell wall

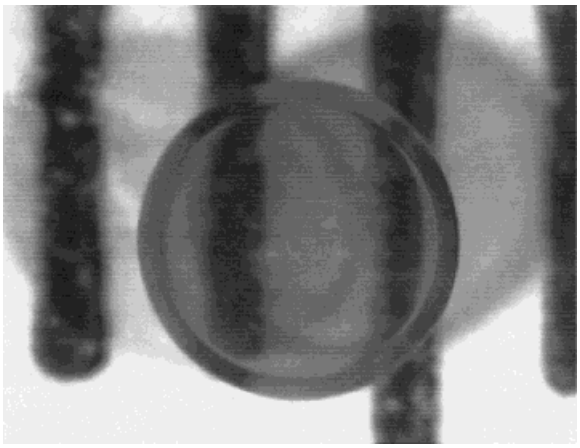

**Figure 12** Photograph of a dry RF foam shell. The diameter, wall thickness, and density of the shell are, respectively, 1.90 mm, 120 $\mu$m, and 63 mg/cm$^3$.

indicate that the density of the foam is uniform throughout and that the foam shows the same submicron cell structure as RF aerogel prepared by conventional means.

## CONCLUSIONS

We have successfully developed a process for fabricating hollow spherical shells made from low-density resorcinol–formaldehyde aerogel. The most notable accomplishments of this work are reductions in gelation time and shell dehydration. The time required to set the macroscopic interparticle gel structure was reduced from several hours to several minutes by adding acid following the base-catalyzed particle growth stage. However, additional annealing of the gel for at least 20 h is needed to maximize intraparticle crosslinking and minimize swelling in exchange solvents. Increasing the molar ratio of formaldehyde to resorcinol from 2 to 3 also helps to reduce swelling and to reduce the shrinkage of the gel upon supercritical $CO_2$ drying. Dehydration of the shells during cure was drastically reduced by prudent selection of immiscible oil phases and by saturating the exterior oil phase with water during the annealing process. The resulting foam shells have densities that approach their theoretical value and the measured density of bulk aerogel of the same formulation.

Two important issues remain with respect to the use of these shells as potential fuel containers for inertial confinement fusion experiments. First, the factors that control shell wall-thickness uniformity must be explored. The only control utilized here is density matching, which essentially limits the position of the interior oil droplet to a random walk within the aqueous RF droplet. We are not cognizant of any naturally occurring centering forces and artificial ones[20] appear difficult to implement. Second, ICF target specifications require that the outside of the shells be coated with a transparent, smooth, full-density polymer layer 5 to 200 $\mu$m thick. We are currently exploring overcoating shells by two methods. The first is deposition of the layer from the vapor phase onto a dry shell using plasma polymerization techniques.[21–23] The second is an interfacial polycondensation technique in the liquid phase (prior to drying) that is similar to that developed by Takagi et al.[6] for methacrylate foam shells.

This work was performed under the auspices of the U.S. Department of Energy by the Lawrence Livermore National Laboratory under Contract No. W-7405-ENG-48 and by W. J. Schafer Associates and Soane Technologies under Contract No. DE-AC03–95SF20732. The authors thank Dr. Richard Pekala for useful discussions concerning RF chemistry.

## APPENDIX—SHELL DEHYDRATION MODEL

Our modeling objective was to qualitatively capture the relevant physics of the dehydration process in order to guide the choice of experimental conditions. Thus, we considered a simplified model in which convectively driven water loss from the preform occurs by quiescent diffusion through an oil phase boundary layer of thickness $\varepsilon$, which depends on the oil phase fluid properties and experimental agitation conditions. The model relies on several justifiable assumptions: (1) the average concentration of water in the exterior oil phase (beyond the boundary layer) is assumed to be unaffected by the water lost from the preform. (2) The concentration of water in the aqueous RF layer is assumed to be uniform because water transport in the aqueous phase is rapid. (3) The water concentration in the oil phase at the interface is assumed to be constant and equal to its initial saturation value. (4) The outer radius of the shell is taken as constant. (5) The interior oil phase does not contribute significantly to the dehydration of the shell because its volume is very small compared to the volume of the exterior oil phase.

As defined, the problem is reduced to the diffusion of water through a spherical oil layer of thickness $\varepsilon$ surrounding an aqueous source of radius $r = R$. For boundary conditions, the concentration of water is set to zero at $r = R + \varepsilon$ and to a constant at the surface of the source, $C(R, t) = C_s$. The transient solution to this problem is available from Crank,[24] but for our purposes the steady-state solution,

$$C(r) = \frac{C_S R}{r}\left\{1 - \frac{r - R}{\varepsilon}\right\} \qquad \text{(A1)}$$

is sufficient. The rate of water loss from the aqueous phase equals the diffusive flux of water at the shell surface, $r = R$, times the area of the shell,

$$\frac{dN(t)}{dt} = -4\pi R^2 D\left(\frac{\partial C}{\partial r}\right)_{r=R} \qquad \text{(A2)}$$

where $N(t)$ is the total amount of water that has left the aqueous phase at time $t$, and $D$ is the diffusivity of water in the oil phase. The fractional rate of water loss can be found by normalizing eq. (A2) by the initial amount of water in the aqueous phase, $N_A \approx 4\pi R^2 \delta C_A$, where $C_A$ is the initial water concentration in the aqueous layer of initial thickness $\delta$. The result is

$$\frac{df}{dt} = \frac{Dk_s}{\delta}\left(\frac{1}{\varepsilon} + \frac{1}{R}\right) \tag{A3}$$

where $f(t)$ ($\equiv N(t)/N_A$) is the fraction of water removed from the aqueous layer at time $t$, and the partition coefficient $k_s$, defined by $C_S = k_s C_A$, governs the equilibrium between water in the oil and aqueous phases at $r = R$. The partition coefficient depends on the temperature and compositions of the coexisting phases and can be estimated by $k_s \approx w_{sat}(\rho/\rho_A)$, where $w_{sat}$ is the mass fraction of water in the saturated oil phase, $\rho$ is the density of the oil phase, and $\rho_A$ is the density of water. Because we have assumed that $C_S$ remains constant as the water content of the aqueous layer decreases, eq. (A3) can incorrectly predict values of $f > 1$. However, for $f < 0.5$ the water concentration in the aqueous phase will still be within 5% of its initial value, and thus eq. (A3) is adequate. The effect of an initial background water concentration can be included by simply replacing the term $Dk_s$ in eq. (A3) with $Dk_s(1 - C_0/C_S)$, where $C_0$ is the initial water concentration in the oil phase.

The boundary layer thickness $\varepsilon$ is estimated from boundary layer theory for laminar flow past a flat plate[25]:

$$\varepsilon = 4.64d\left(\frac{\mu}{dv\rho}\right)^{1/2}\left(\frac{D\rho}{\mu}\right)^{1/3} \tag{A4}$$

where $\mu$ is the viscosity of the oil phase, $v$ is the flow velocity far from the plate, and $d$ is a characteristic distance for fluid flow along the plate. Although it is strictly incorrect to use the flat plate solution for flow past a sphere, as long as $\varepsilon \ll R$, this equation should provide a reasonable approximation with $d = R$.

Finally, the diffusivity of water in the oil phase needs to be expressed in terms of fundamental fluid properties. In our quantitative work with this model, we found that the empirical Wilke-Chang equation[26] generally gave satisfactory estimates for the diffusivity of water in various organic solvents. This correlation provides the following relationship among $D$, the temperature $T$, and the solvent viscosity and molecular weight $M$:

$$D \propto \frac{TM^{1/2}}{\mu}. \tag{A5}$$

In the thin boundary layer limit, $\varepsilon \ll R$, the explicit dependence of the fractional rate of water loss on solvent properties and processing conditions can be obtained by substituting eq. (A4) for $\varepsilon$ and eq. (A5) for $D$ in eq. (A3). This yields

$$\frac{df}{dt} \propto \frac{k_s T^{2/3} M^{1/3} v^{1/2} \rho^{1/6}}{\delta \mu^{5/6} R^{1/2}} \propto \frac{k_s T^{2/3} \omega^{1/2}}{\delta \mu^{5/6}}. \tag{A6}$$

On the far right the relatively weak oil phase $M$ and $\rho$ dependencies are suppressed and the relevant velocity difference $v$ between the shell surface and the outer edge of the boundary layer is recognized as being proportional to $\omega(R + \varepsilon) \approx \omega R$, where $\omega$ is a measure of the local oil phase velocity gradient and is dependent upon the method and degree of solution agitation.

## REFERENCES


1. S. W. Haan et al., *Phys. Plasmas,* **2,** 2480 (1995).
2. S. Lindl, *Phys. Plasmas,* **2,** 3933 (1995).
3. R. A. Sacks and D. H. Darling, *Nucl. Fusion,* **27,** 447 (1987).
4. C. Chen, T. Norimatsu, M. Takagi, H. Katayama, T. Yamanaka, and S. Nakai, *J. Vac. Sci. Technol. A,* **9,** 340 (1991).
5. M. Takagi, T. Norimatsu, T. Yamanaka, S. Nakai, and H. Ito, *J. Vac. Sci. Technol. A,* **9,** 820 (1991).
6. M. Takagi, M. Ishihara, T. Norimatsu, T. Yamanaka, Y. Izawa, and S. Nakai, *J. Vac. Sci. Technol. A,* **11,** 2837 (1993).
7. T. Norimatsu, C. M. Chen, K. Nakajima, M. Takagi, Y. Izawa, T. Yamanaka, and S. Nakai, *J. Vac. Sci. Technol. A,* **12,** 1293 (1994).
8. M. Takagi, T. Norimatsu, Y. Izawa, and S. Nakai, *MRS Symp. Proc.,* **372,** 199 (1995).
9. D. Schroen-Carey, G. E. Overturf, III, R. Reibold, S. R. Buckley, S. A. Letts, and R. Cook, *J. Vac. Sci. Technol. A,* **13,** 2568 (1995).
10. G. E. Overturf, III, R. Cook, S. A. Letts, S. R. Buckley, M. R. McClellan, and D. Schroen-Carey, *Fusion Technol.,* **28,** 1803 (1995).
11. R. B. Stephens, *Fusion Technol.,* **28,** 1809 (1995).
12. R. W. Pekala, C. T. Alviso, and J. D. LeMay, in *Chemical Processing of Advanced Materials,* L. L.

Hench and J. K. West, eds., Wiley, New York, 1992, p. 671.
13. R. W. Pekala, *J. Mater. Sci.,* **24,** 3221 (1989).
14. R. W. Pekala, C. T. Alviso, F. M. Kong, and S. S. Hulsey, *J. Non-Cryst. Solids,* **145,** 90 (1992).
15. S. A. Letts, S. R. Buckley, F. M. Kong, E. F Lindsey, and M. L. Sattler, *Mater. Res. Soc. Symp.,* **177,** 275 (1990).
16. R. W. Pekala and F. M. Kong, *Rev. Phys. Appl. Suppl.,* **4,** 24 (1989).
17. P. M. Cotts and R. W. Pekala, *Polym. Preprints,* **32,** 451 (1991).
18. P. M. Cotts, in *Synthesis, Characterization, and Theory of Polymeric Networks and Gels,* S. M. Aharoni, Ed., Plenum Press, New York, 1992, p. 41.
19. J. A. Riddick, W. B. Bunger, and T. K. Sakano, *Organic Solvents: Physical Properties and Methods of Purification,* John Wiley & Sons, New York, 1986, p. 442.
20. C. P. Lee and T. G. Wang, *J. Fluid Mech.,* **188,** 411 (1988).
21. G. W. Collins, S. A. Letts, E. M. Fearon, R. L. McEachern, and T. P. Bernat, *Phys. Rev. Lett.,* **73,** 708 (1994).
22. S. A. Letts, D. E. Miller, R. A. Corley, T. M. Tillotson, and L. A. Witt, *J. Vac. Sci. Technol. A,* **3,** 1277 (1985).
23. S. A. Letts, D. W. Myers, and L. A. Witt, *J. Vac. Sci. Technol.,* **19,** 739 (1981).
24. J. Crank, *The Mathematics of Diffusion,* Oxford Univ. Press, London, 1957, p. 95.
25. E. L. Cussler, *Diffusion: Mass Transfer in Fluids Systems,* Cambridge Univ. Press, Cambridge, 1984, p. 294.
26. C. R. Wilke and P. C. Chang, *AIChE J.,* **1,** 264 (1955); also ref. 25, p. 121.